ISSN: 2710-XXXX DOI: 10.XXXX/jstit.202107_1(1).0001

Influence of Voltage Fluctuation on Dynamic Characteristics of Traction Drive System for Rail Vehicle

Xun Wang[1, *], Pingbo Wu[1]

[1] State Key Laboratory of Traction Power, Southwest Jiaotong University, Chengdu, Sichuan, China

[*] Corresponding Author, wangxun0323@126.com

Abstract

With the increase of traffic pressure caused by the increase of urban population in recent years, rail transit has developed rapidly in major cities because of its advantages of quickness, safety and convenience. Traction drive system is the key subsystem of rail transit vehicles. It drives the train to travel and brake through electromechanical coupling integrated control, which determines the train running speed, power quality and comfort. In this work, a vehicle electromechanical coupling dynamic model was established to analyse the influence of voltage fluctuation on dynamic characteristics of traction drive system. The results show that without considering the track excitation and 1500V DC power supply voltage, when the voltage amplitude increases, the vibration of the transmission system increases significantly. When the voltage amplitude decreases, the longitudinal vibration of the transmission system decreases significantly, the lateral vibration of the transmission system decreases slightly, the motor decreases significantly and the gearbox decreases slightly in the vertical vibration of the transmission system.

Keywords

Traction drive system; Electro-mechanical coupling; Dynamic characteristics; Rail vehicle

1 Introduction

As the core component to realize train traction and braking operation, metro traction drive system [1-3] is mainly composed of intermediate DC link, traction inverter, traction motor, gear drive system, etc. The metro traction drive system outputs DC to the traction inverter through the intermediate DC link. The traction inverter outputs three-phase AC with adjustable voltage and frequency to the traction asynchronous motor. The torque and speed output by the shaft end of the traction motor are transmitted to the wheel set through the gear system and converted into rim traction force [4-6] and linear speed.

ISSN: 2710-XXXX DOI: 10.XXXX/jstit.202107_1(1).0001

During the operation of the subway, the train speed is adjusted by adjusting the speed of the traction motor, which is adjusted by the voltage output by the traction inverter and the three-phase AC with controllable frequency. With the rapid development of power electronic switching devices, VVVF variable frequency speed regulation system has been widely used. It adopts sinusoidal pulse width modulation (SPWM) technology, which can effectively adjust voltage and frequency. The Metro adopts DC power supply and outputs AC power to the traction motor through the traction inverter. At present, the traction inverter mainly adopts SPWM control technology to realize the regulation of AC voltage and frequency, and then realize the regulation of traction motor speed, so as to further realize the regulation of metro train speed.

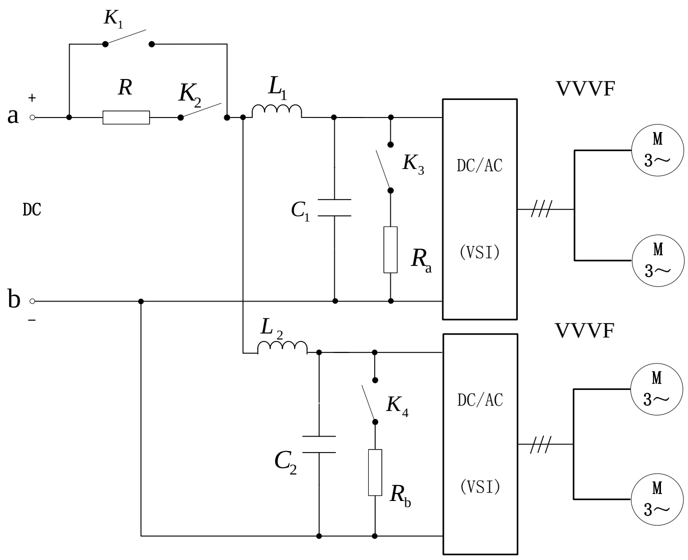

Fig. 1 Brief diagram for electric traction drive system of subway.

Metro traction drive system [7-10] is shown in Fig. 1, which is mainly composed of intermediate DC link, traction inverter, traction motor, gear drive system, etc. Under the traction condition of metro train, the traction motor is in the motor state. The DC obtained from the third rail or catenary is output to the traction inverter through the intermediate DC link. The inverter adopts SPWM technology to convert the DC into three-phase AC with controllable voltage and frequency, which is output to the traction asynchronous motor. The motor converts the obtained electric energy into mechanical energy to drive the metro train forward. Under the braking condition of metro train, the traction motor is in the power generation state. The traction inverter converts the three-phase AC output by the traction motor into DC and returns to the power grid through the intermediate DC link, that is, regenerative braking can be realized. DC can also dissipate heat and energy through resistance, that is, resistance braking can be realized.

ISSN: 2710-XXXX DOI: 10.XXXX/jstit.202107_1(1).0001

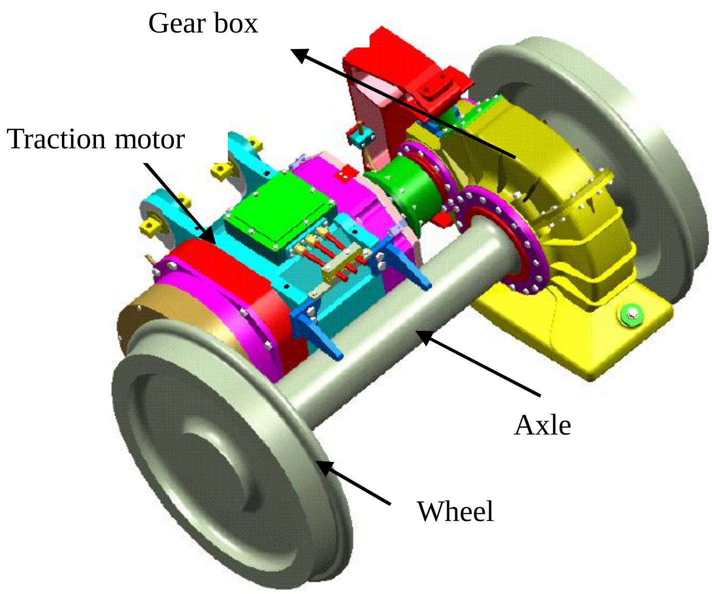

Fig. 2 Mechanical transmission of traction drive system for rail transit.

The traction motor could convert electric energy into mechanical energy and output electromagnetic torque, shown in Fig. 2, which could be transmitted to the axle through the gear system to drive the wheel-set to rotate, so as to drive the train forward. During the operation of metro vehicles, the amplitude of DC power supply voltage could fluctuate. When 1500V DC power supply voltage is adopted, the fluctuation range is 1000~1800V. Voltage fluctuation could cause motor torque fluctuation, and then affect the vibration characteristics of the transmission system [11-13] for rail transit.

2 Establishment of Electro-mechanical Coupling Simulation Model

The direct torque control model of motor is established by using Simulink simulation platform, and the dynamic model of Metro motor car is established by using SIMPACK simulation software. On this basis, the mechanical-electrical coupling simulation model considering traction transmission systems [14] such as motor, rotor, big gear and pinion is established by using joint simulation method.

The direct torque control technology uses the space vector analysis method to calculate and control the motor torque directly in the stator coordinate system. The stator magnetic field orientation is adopted, and the PWM wave signal is generated with the help of discrete two-point regulation to directly control the switching state of the inverter, so as to obtain the high dynamic performance of the torque.

Direct torque control is a direct control of the switching state of the inverter by comparing the measured values of the flux linkage and torque to the observed values. Therefore, in order to achieve feedback control in the direct torque control system, the current stator flux linkage and torque need to be accurately estimated.

The estimation of the stator flux linkage is as follows:

$$\begin{cases} \psi_{s\alpha} = \int (u_{s\alpha} - i_{s\alpha} R_s) dt \\ \psi_{s\beta} = \int (u_{s\beta} - i_{s\beta} R_s) dt \end{cases} \tag{1}$$

ISSN: 2710-XXXX DOI: 10.XXXX/jstit.202107_1(1).0001

The electromagnetic torque can be expressed as

$$T_{\mathrm{e}} = n_{\mathrm{p}} \vec{\psi}_{\mathrm{s}} \times \vec{i}_{\mathrm{s}} \tag{2}$$

Where: $\vec{\psi}_{\mathrm{s}}$—Stator flux linkage space vector of three phase shafting; $\vec{i}_{\mathrm{s}}$—Stator current space vector of three phase shafting.

The observational value of the electromagnetic torque could be obtained by the formula (2):

$$T_{\mathrm{e}} = n_{\mathrm{p}} (\hat{\psi}_{\mathrm{s}\alpha} i_{\mathrm{s}\beta} - \hat{\psi}_{\mathrm{s}\beta} i_{\mathrm{s}\alpha}) \tag{3}$$

Where: $\hat{\psi}_{\mathrm{s}\alpha}$, $\hat{\psi}_{\mathrm{s}\beta}$—Estimated value; $i_{\mathrm{s}\alpha}$, $i_{\mathrm{s}\beta}$—Measured value.

When establishing the model of metro motor car system [15-17], the stator and body of traction motor are considered as a whole, which are connected with the frame through three rubber nodes. The motor rotor is an individual and rotates relative to the motor stator. The large and small gears of gearbox have an independent degree of freedom relative to the box, and the pinion and pinion shaft are considered as a whole. The large gear is consolidated with the axle by constraints, and the torque transmission between the large and small gears is simulated by constraints. One end of the gearbox adopts a rotary hinge, which has an independent degree of freedom relative to the axle, and the other end uses force element to simulate the elastic connection between the suspender and the frame. Metro power vehicle system as shown in Fig. 3 consists of 4 wheel-sets, 8 axle boxes, 4 gear boxes, 4 pairs of gears, 4 motors, 4 motor rotors, 2 frames and 1 vehicle body.

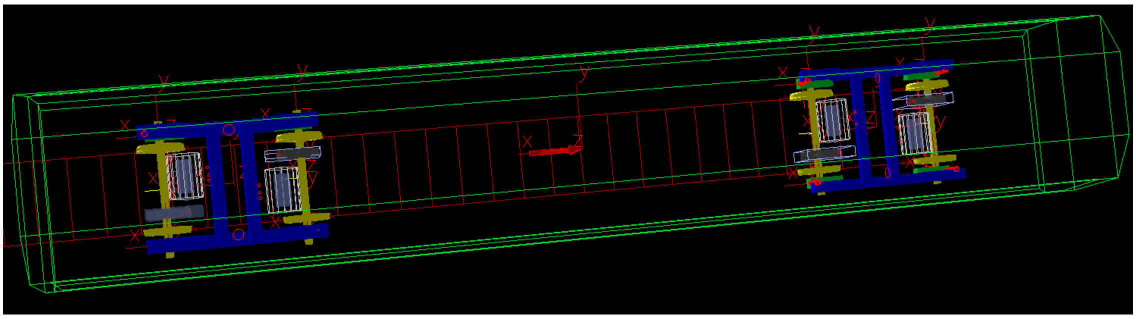

Fig. 3 Vehicle model with traction drive system for rail transit.

During simulation for electromechanical coupling [18, 19], as shown in Fig. 4, given a desired motor rotor speed, the output current motor rotor speed could be compared with it. If the expected value is larger, the positive electromagnetic torque will be output, and the SIMPACK motor rotor speed will become larger. If the expected value is smaller, the negative electromagnetic torque will be output, and the SIMPACK motor rotor speed will become smaller. If the two values are equal, then the output electromagnetic torque is the motor load torque, and the running resistance of the train changes with the change of speed.

ISSN: 2710-XXXX DOI: 10.XXXX/jstit.202107_1(1).0001

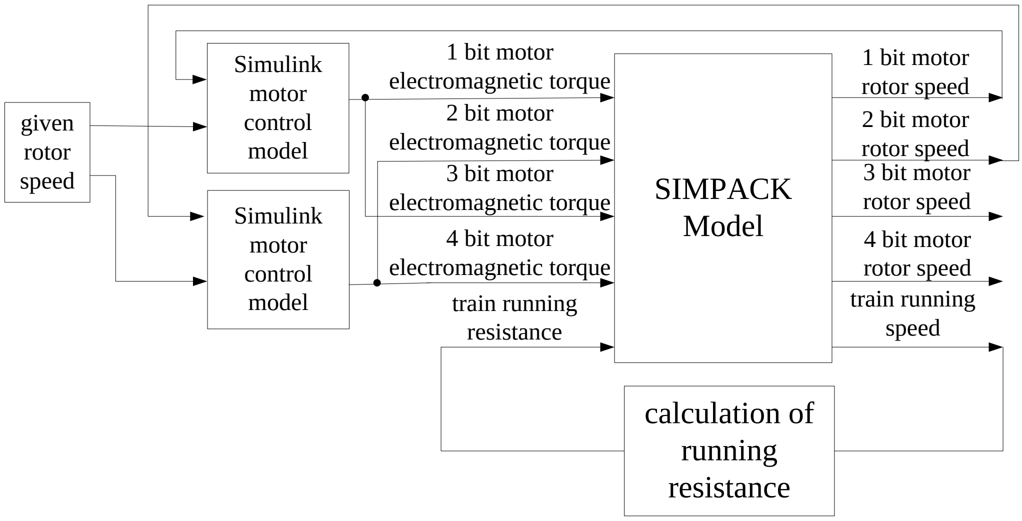

Fig. 4 Block diagram of electromechanical coupling model for rail transit.

3 Results and Discussions

In order to study the influence of voltage fluctuation on the transmission system, the DC power supply voltage was set to 1500V, 1200V and 1800V, respectively, the running speed was 60km/h, and the vibration acceleration of motor and gearbox in longitudinal, lateral and vertical directions was simulated respectively. In SIMPACK Metro model, the track was a straight track without track spectrum, The simulation step of Simulink model was 0.0001s, and the simulation frequency range was 0~2000Hz. The 5S data was intercepted for Fourier transform to obtain the spectrum results, and the results were analysed.

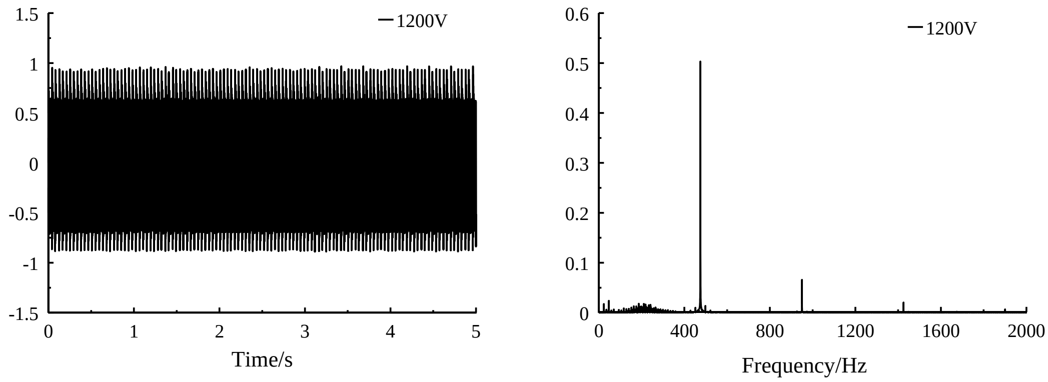

ISSN: 2710-XXXX DOI: 10.XXXX/jstit.202107_1(1).0001

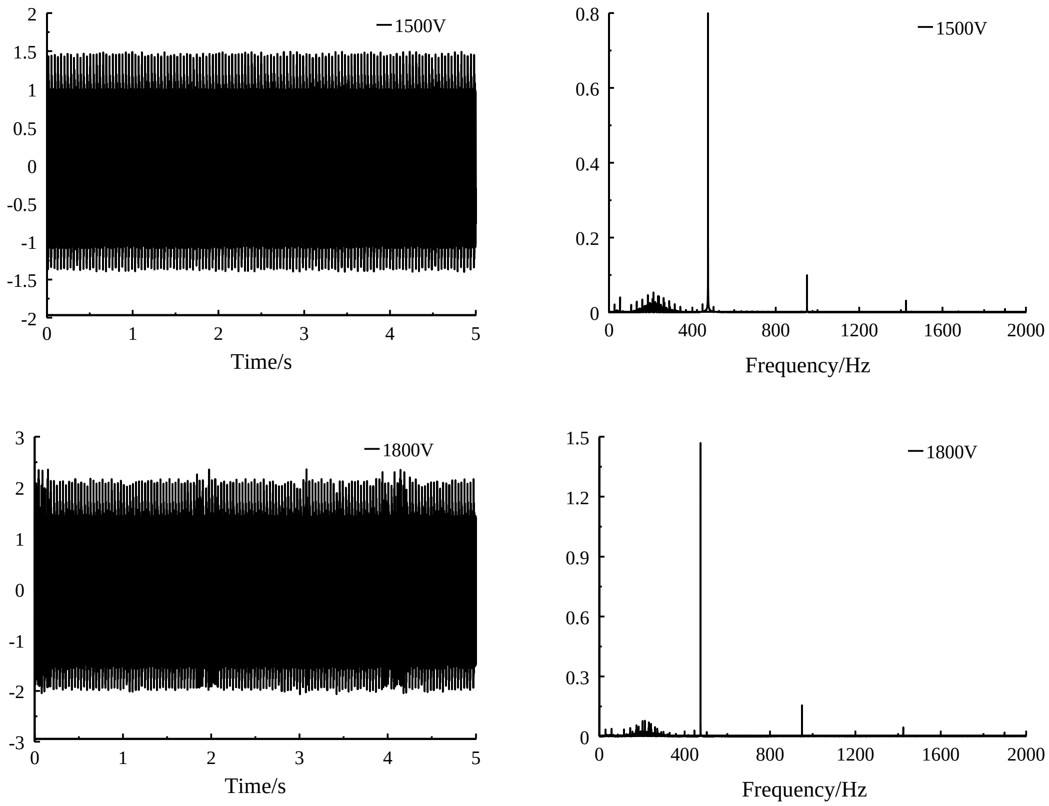

Fig. 5 Motor longitudinal vibration acceleration.

It can be found from Fig. 5 that when the DC supply voltage is reduced, the longitudinal vibration amplitude of the motor decreases correspondingly, while the vibration amplitude increases with the increase of voltage. It can be seen from the frequency domain diagram that the frequency domain distribution of the longitudinal vibration of the motor under different voltages is the same. But the larger the amplitude of the DC supply voltage, the greater the longitudinal vibration amplitude of the motor. In particular, the amplitude of the 12 times frequency of the rotor fundamental wave increases obviously when the supply voltage is increased.

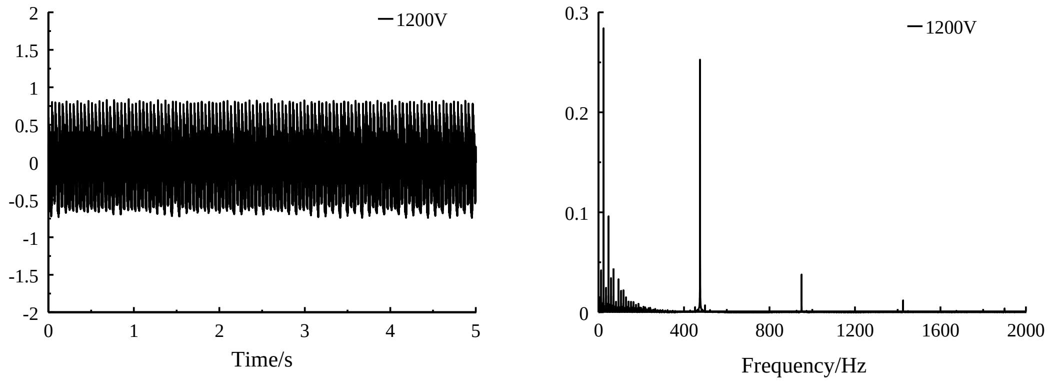

ISSN: 2710-XXXX DOI: 10.XXXX/jstit.202107_1(1).0001

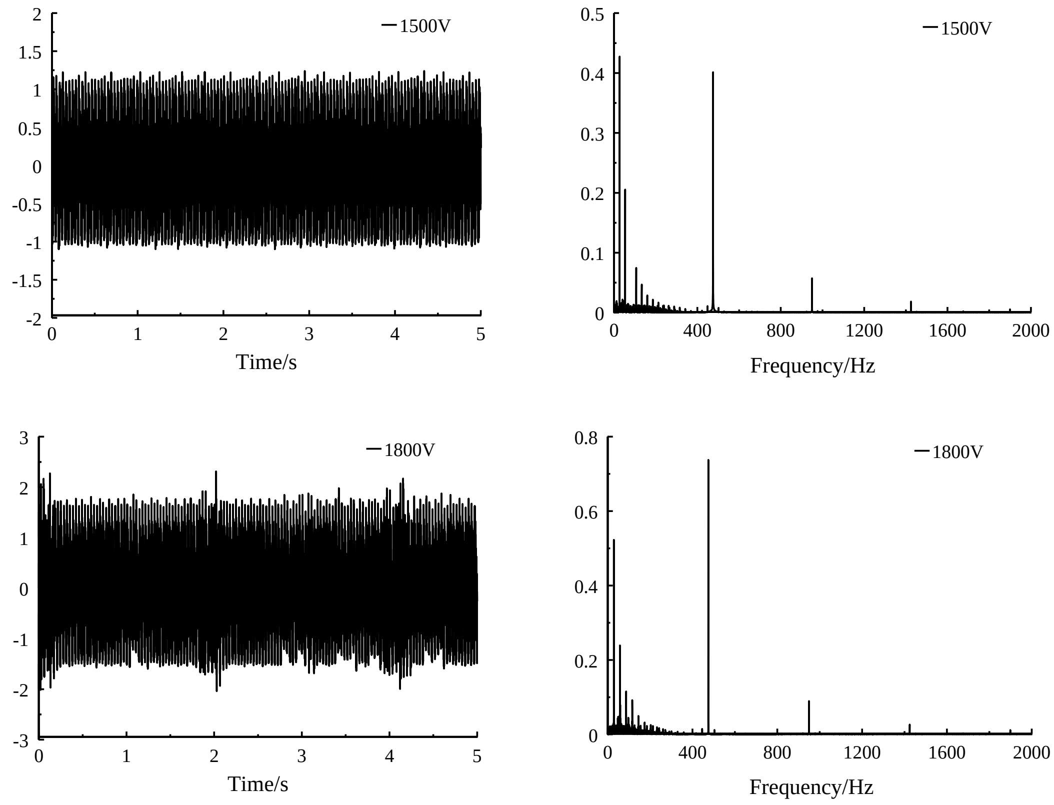

Fig. 6 Gear box longitudinal vibration acceleration.

Fig. 6 shows that the larger the amplitude of the DC supply voltage, the greater the longitudinal vibration amplitude of the gear box. In particular, the amplitude of the 12 times frequency of the rotor fundamental wave increases obviously when the supply voltage is increased. It is indicated that the longitudinal vibration of the gear box will also increase when the supply voltage is increased under 1500V DC power supply. When the supply voltage is reduced, the longitudinal vibration of the gear box will decrease.

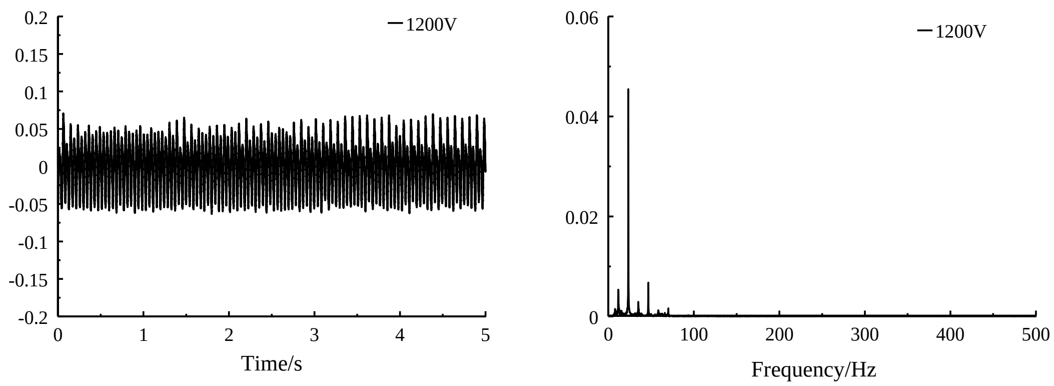

ISSN: 2710-XXXX DOI: 10.XXXX/jstit.202107_1(1).0001

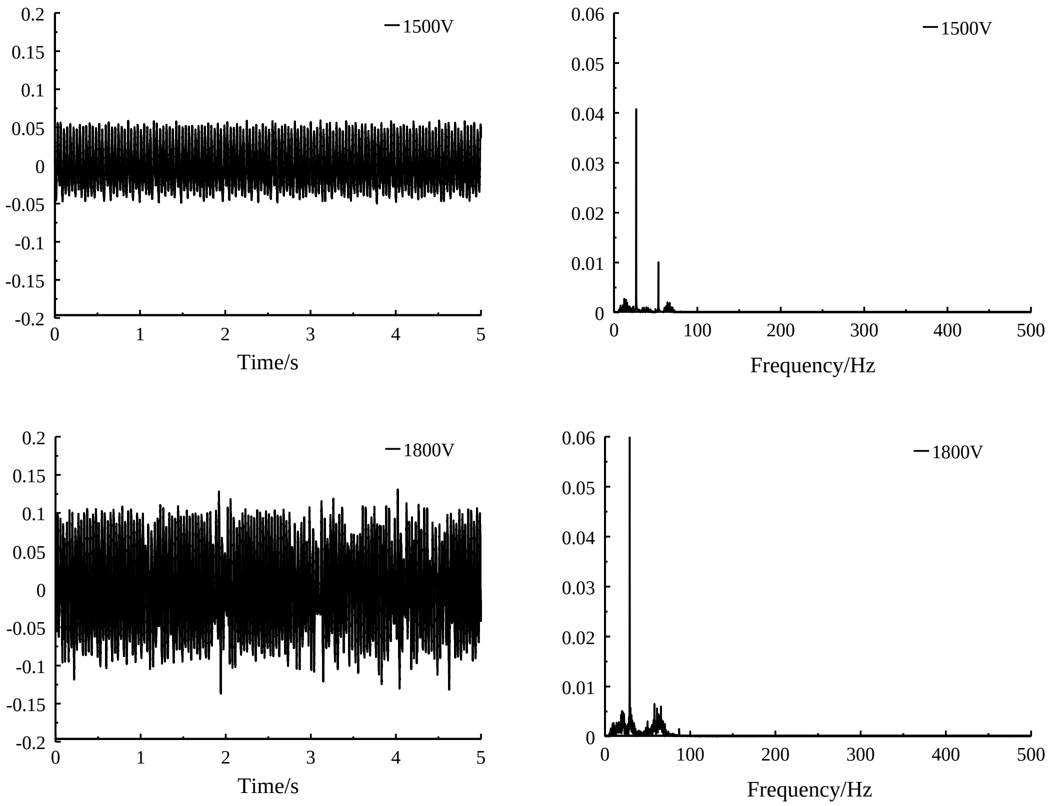

Fig. 7 Motor lateral vibration acceleration.

It can be seen from the frequency domain diagram from Fig. 7 that the frequency domain distribution of the lateral vibration of the motor under different voltages is the same. When 1500V power supply is applied, the lateral vibration of the motor will also increase when the supply voltage is increased. When the supply voltage is reduced, the lateral vibration of the motor will not change much.

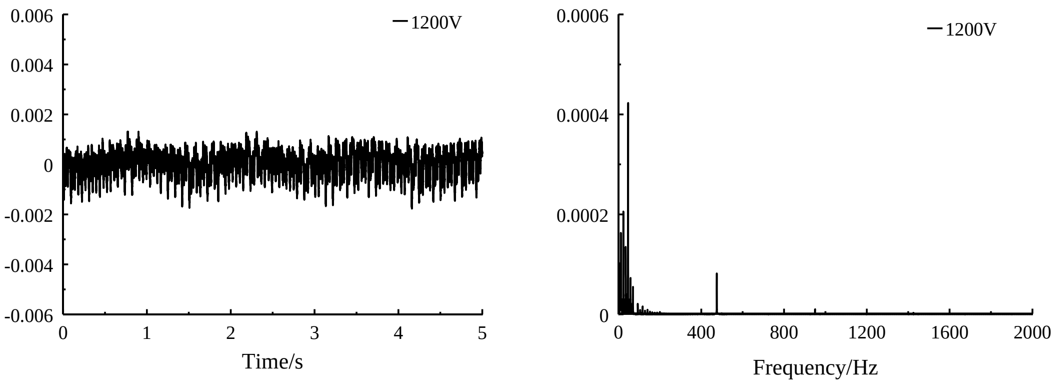

ISSN: 2710-XXXX DOI: 10.XXXX/jstit.202107_1(1).0001

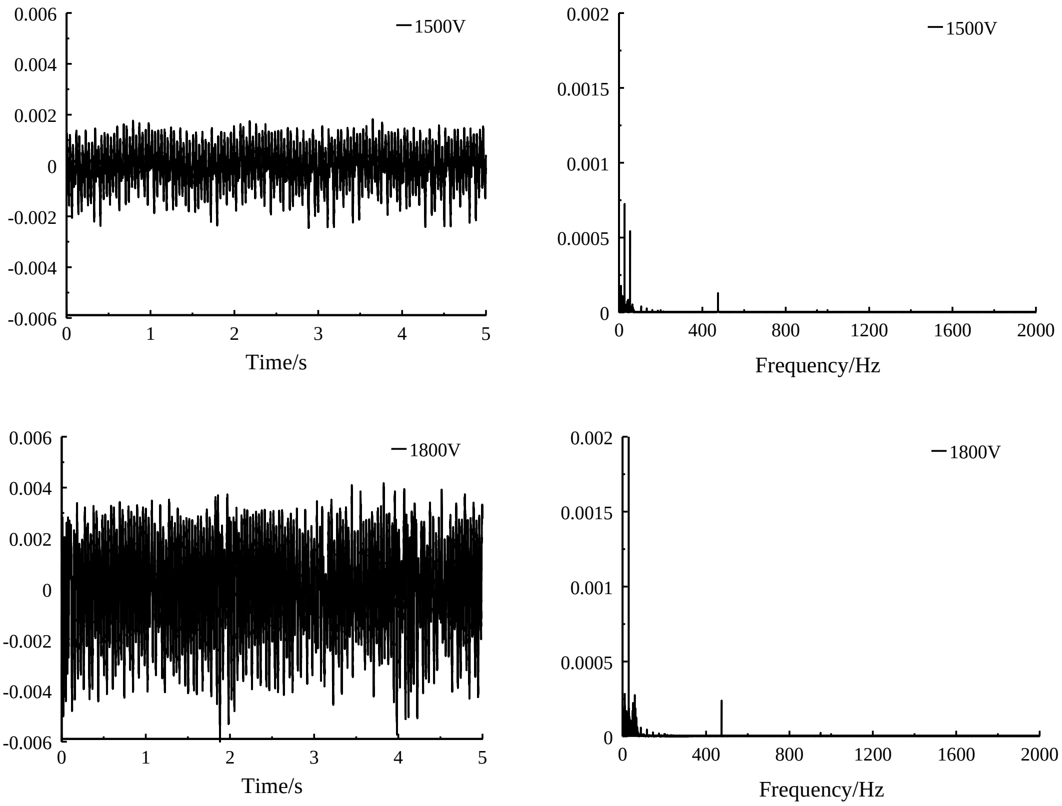

Fig. 8 Gear box lateral vibration acceleration.

As can be seen from Fig. 8, the higher the voltage, the greater the vibration acceleration amplitude of the gearbox. As can be seen from the frequency domain diagram, the vibration frequency is mainly below 100Hz.

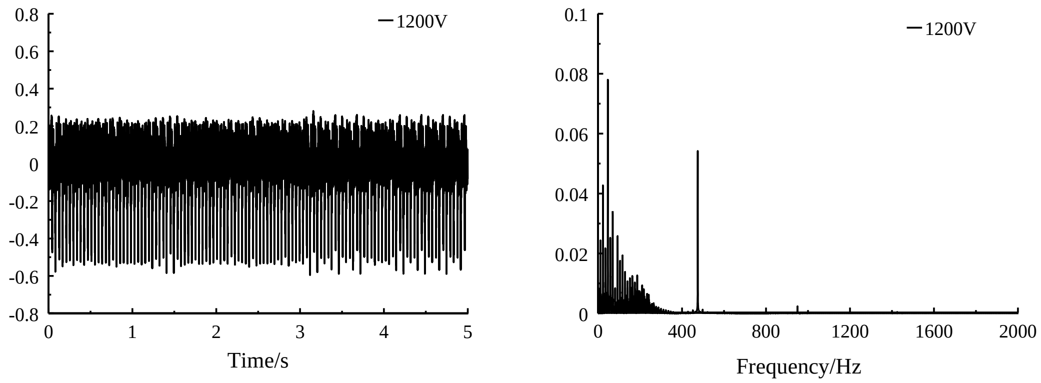

ISSN: 2710-XXXX DOI: 10.XXXX/jstit.202107_1(1).0001

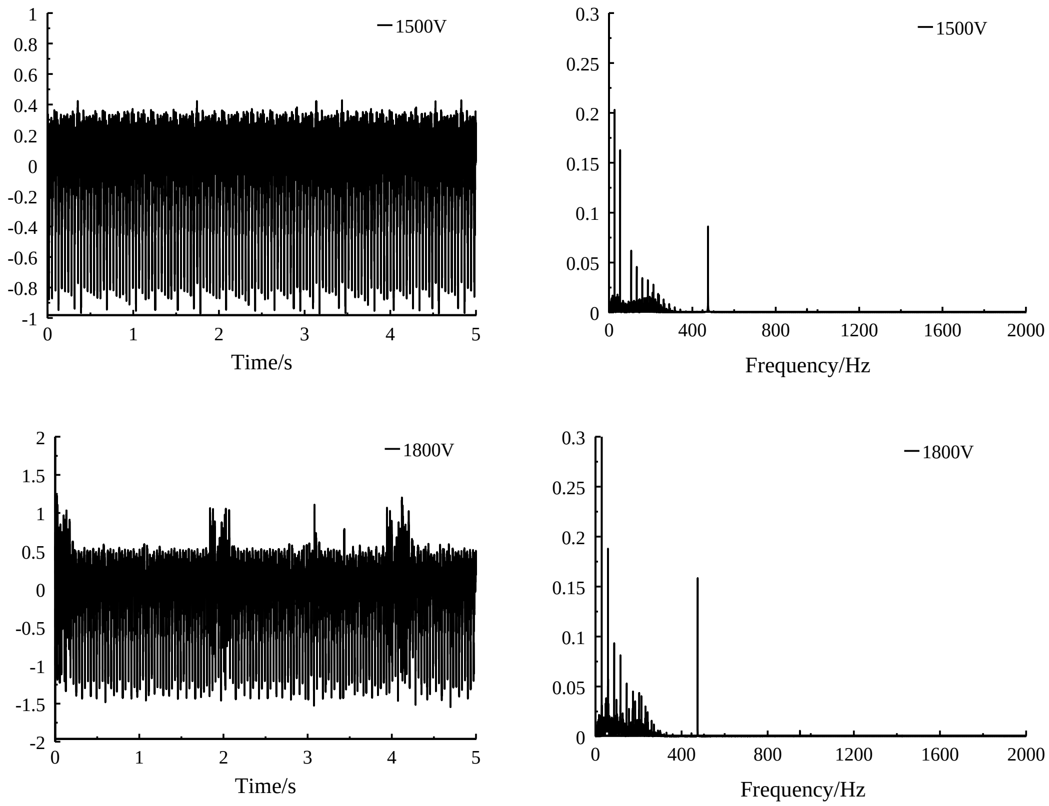

Fig. 9 Motor vertical vibration acceleration.

Fig. 9 shows that the vertical vibration amplitude effect of voltage increase on the motor is larger than that of the voltage reduction. It can be seen from the frequency domain diagram that the larger the amplitude of the DC supply voltage, the greater the vertical vibration amplitude of the motor.

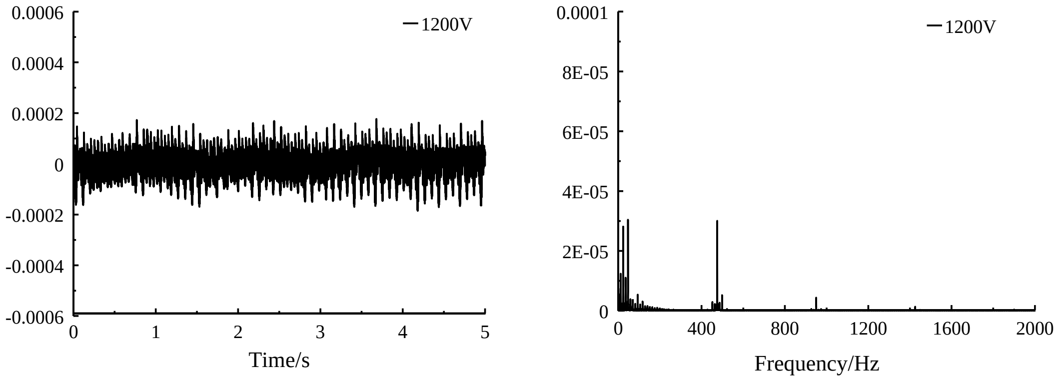

ISSN: 2710-XXXX DOI: 10.XXXX/jstit.202107_1(1).0001

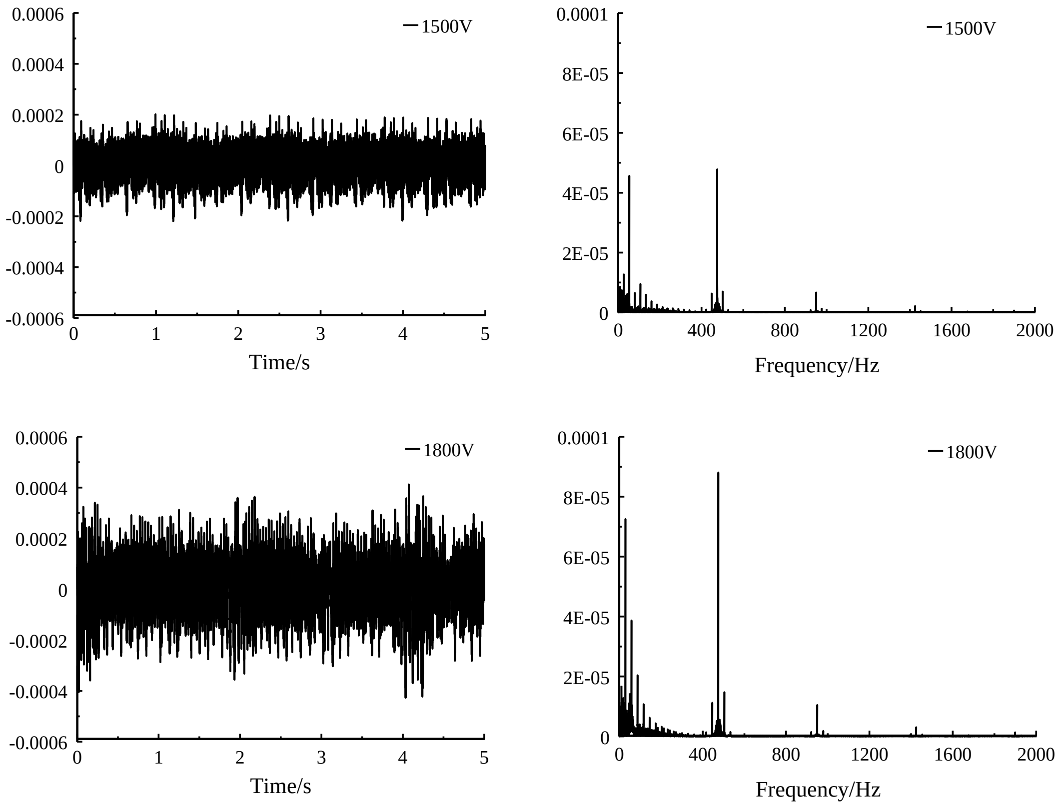

Fig. 10 Gear box vertical vibration acceleration.

The time domain diagram and frequency domain diagram of the vertical vibration acceleration for the gear box are shown in shown in Fig. 10 at three voltages. It can be seen in time-domain diagram that the vertical vibration amplitude of gearbox is very small. With the change of voltage, the vibration amplitude changes accordingly.

4 Conclusions

As an important component of train speed regulation, traction transmission system is the power source and the main transmission component of traction force. Its dynamic characteristics could affect the dynamic performance of vehicle system to a certain extent. With the rapid development of high-speed railway, the running speed of the train continues to improve, the dynamic characteristic of the vehicle is more complex, and the influence of the electrical part of the traction transmission system gradually appears. The motor and gearbox are the important components of the train power bogie to complete the conversion and transmission of electric energy to mechanical energy, and their dynamic characteristics are most directly and obviously affected by the electrical characteristics of the traction system. The simulation results show that under the DC 1500V power supply voltage, when the voltage amplitude increases, the longitudinal, lateral and vertical vibration of the transmission system increases significantly. When the voltage amplitude decreases, the longitudinal vibration of the transmission system decreases significantly, the lateral vibration of the transmission system decreases slightly, the motor decreases significantly and the gearbox decreases slightly in the vertical vibration of the transmission system.

ISSN: 2710-XXXX DOI: 10.XXXX/jstit.202107_1(1).0001

Acknowledgements

The financial support of national Natural Science Foundation of China (U1934202) is gratefully acknowledged.

References

1. An ThiHoai Thu Anh and Vu Hoang Phuong, *Braking energy recuperation for electric traction drive in urban rail transit network based on control super-capacitor energy storage system.* Journal of Electrical Systems, 2018. **14**(3): 99-114.
2. Chen Zhiwen, Li Xueming, Yang Chao, Peng Tao, Yang Chunhua, Karimi H. R., *A data-driven ground fault detection and isolation method for main circuit in railway electrical traction system.* Isa Transactions, 2019. **87**: 264-271.
3. Feng Jianghua, Shang Jing, Zhang Zhixue, Liu Huadong, and Huang Zihao, *Solid-state transformer-based new traction drive system and control.* Frontiers of Mechanical Engineering, 2018. **13**(3): 411-426.
4. Fukui Rui, Okabe Taira, Nakao Masayuki, and Honda Yukihiro, *Highly efficient traction drive system with a normal force controller using a piezoelectric actuator.* Advances in Mechanical Engineering, 2017. **9**(10).
5. Wang Huimin, Ge Xinglai, and Liu Yong-Chao, *An Active Damping Stabilization Scheme for the Suppression of the DC-Link Oscillation in Metro Traction Drive System.* Ieee Transactions on Industry Applications, 2018. **54**(5): 5113-5123.
6. Yang Chunhua, Yang Chao, Peng Tao, Yang Xiaoyue, and Gui Weihua, *A Fault-Injection Strategy for Traction Drive Control Systems.* Ieee Transactions on Industrial Electronics, 2017. **64**(7): 5719-5727.
7. Dolecek Radovan, Cerny Ondrej, Novak Jaroslav, and Bartlomiejczyk Mikolaj, *Interference in Power system for traction drive with PMSM.* Przeglad Elektrotechniczny, 2012. **88**(9A): 204-207.
8. Dybkowski Mateusz, Orlowska-Kowalska Teresa, and Tarchala Grzegorz, *Sensorless Traction Drive System with Sliding Mode and MRAS(CC) Estimators using Direct Torque Control.* Automatika, 2013. **54**(3): 329-336.
9. Dybkowski Mateusz, Tarchala Grzegorz, and Orlowska-Kowalska Teresa, *Experimental analysis of the sensorless traction drive system with DTC-SVM algorithm and MRAS(CC) estimator.* Przeglad Elektrotechniczny, 2012. **88**(12A): 62-65.
10. Dybkowski Mateusz, Tarchala Grzegorz, Orlowska-Kowalska Teresa, and Kazmierkowski Marian P., *Analysis of the sensorless traction drive system with sliding mode observer.* Przeglad Elektrotechniczny, 2012. **88**(6): 216-220.
11. Golabi Samko, Babaei Ebrahim, Sharifian Mohammad Bagher Bannae, and Golabi Zahed, *Application of Speed, Rotor Flux, Electromagnetic, Load Torque Observers and Diagnostic System in a Vector-Controlled High-Power Traction Motor Drive.* Arabian Journal for Science and Engineering, 2014. **39**(4): 2979-2996.
12. Gou Bin, Ge Xinglai, Wang Shunliang, Feng Xiaoyun, Kuo James B., and Habetler Thomas G., *An Open-Switch Fault Diagnosis Method for Single-*

ISSN: 2710-XXXX DOI: 10.XXXX/jstit.202107_1(1).0001

Phase PWM Rectifier Using a Model-Based Approach in High-Speed Railway Electrical Traction Drive System. IEEE Transactions on Power Electronics, 2016. **31**(5): 3816-3826.

13. Kulworawanichpong T. and Goodman C. J., *Optimal area control of AC railway systems via PWM traction drives.* Iee Proceedings-Electric Power Applications, 2005. **152**(1): 33-40.
14. Pessina G. and Peirone M., *Innovative traction systems for railway transit.* Elettrotecnica, 1992. **79**(12): 1211-1215.
15. Reyhart Delon R. and Anwar Sohel, *Optimal control of an On-Demand All-Wheel Drive system (ODAWD) for vehicle traction enhancement.* International Journal of Vehicle Design, 2011. **56**(1-4): 270-298.
16. Stana Girts, Brazis Viesturs, and Apse-Apsitis Peteris, *Simulation of Induction Traction Drive with Supercapacitor Energy Storage System Test Bench.* Electrical Control and Communication Engineering, 2015. **9**(1): 14-22.
17. Taniguchi Shun, Yasui Kazuya, Yuki Kazuaki, Nakazawa Yosuke, and Onda Shouji, *A Restart Control Method for Position Sensorless PMSM Drive Systems Without Potential Transformer for Railway Vehicle Traction.* Electrical Engineering in Japan, 2015. **193**(3): 44-53.
18. Geng Y. B., *Electromechanical coupled dynamics of rails for electromagnetic launcher*. International Journal of Applied Electromagnetics and Mechanics, 2013. **42**(3): 369-389.
19. Xu L. Z. and Wu D. W., *Electromechanical coupled nonlinear dynamics of euler beam rails for electromagnetic railgun.* Smart Structures and Systems, 2017. **19**(2): 213-224.